Supporting Information

Accelerated Non-Enzymatic Fatty Acid Esterification During Microdroplet Collision: A Method for Enhanced Sustainability

*Pallab Basuri†, Jenifer Shantha Kumar†, Subhashree Das†, and Thalappil Pradeep†**

† DST Unit of Nanoscience (DST UNS) and Thematic Unit of Excellence (TUE), Department of Chemistry, Indian Institute of Technology Madras, Chennai 600036, India.

* Corresponding author

Thalappil Pradeep − DST Unit of Nanoscience (DST UNS) and Thematic Unit of Excellence (TUE), Department of Chemistry, Indian Institute of Technology Madras, Chennai-600 036, India; orcid.org/0000-0003-3174-534X;

Email: pradeep@iitm.ac.in

This supporting information contains:

- 28 pages (S1-S28)

- 26 figures (Figure S1-S26)

- 1 scheme (Scheme S1)

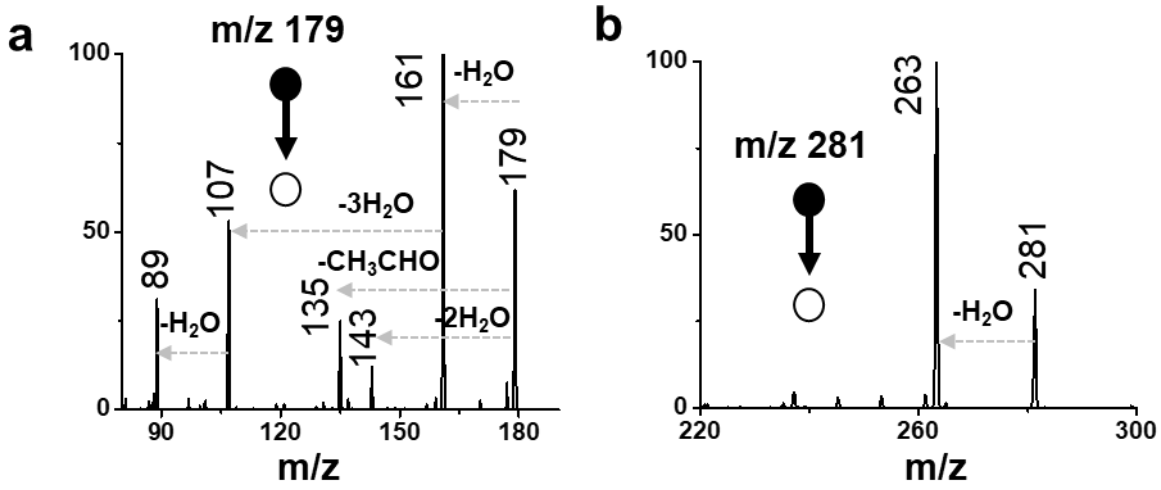

Figure S1. MS/MS spectrum of isolated peaks of a) glucose and b) oleic acid in negative ion mode.

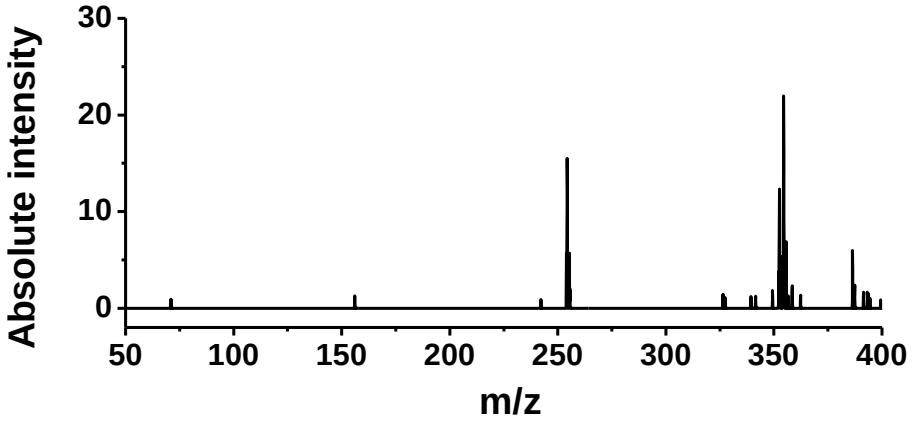

Figure S2. Mass spectrum collected from a nebulized spray of oleic acid in toluene. No potential was applied for the spray. The peaks observed here have absolute intensity lower than 30, while a typical spectrum shows intensity in the range of 10^5-10^6. The origin of such low intense peaks could be due to chemical or electronic noise from the instrument. We did not observe any peak corresponding to deprotonated oleic acid at m/z 281.

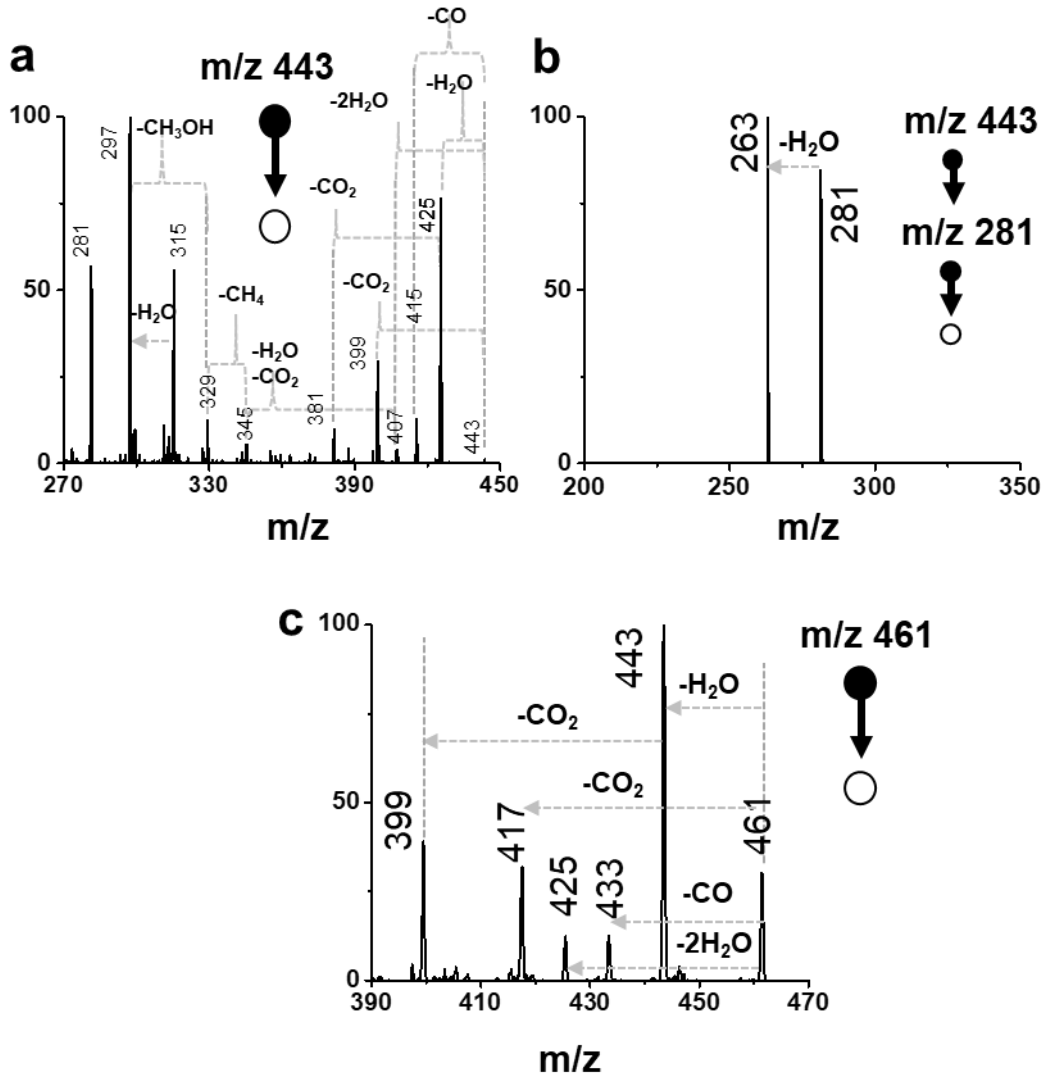

Figure S3. MS/MS and MS/MS/MS mass spectra of m/z (a), 443 (b), 281and (c) 461 in negative ion mode. The noise in the spectra is due to low signal intensities during ion isolation.

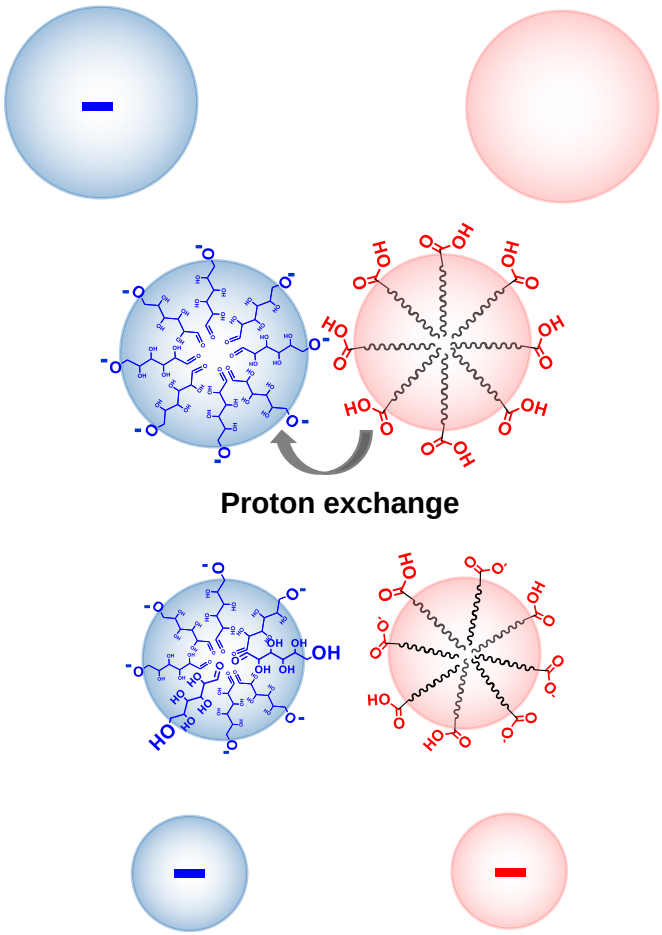

Scheme S1. Schematic illustration of microdroplet collision, showing proton exchange at the interface making both the droplets negatively charged.

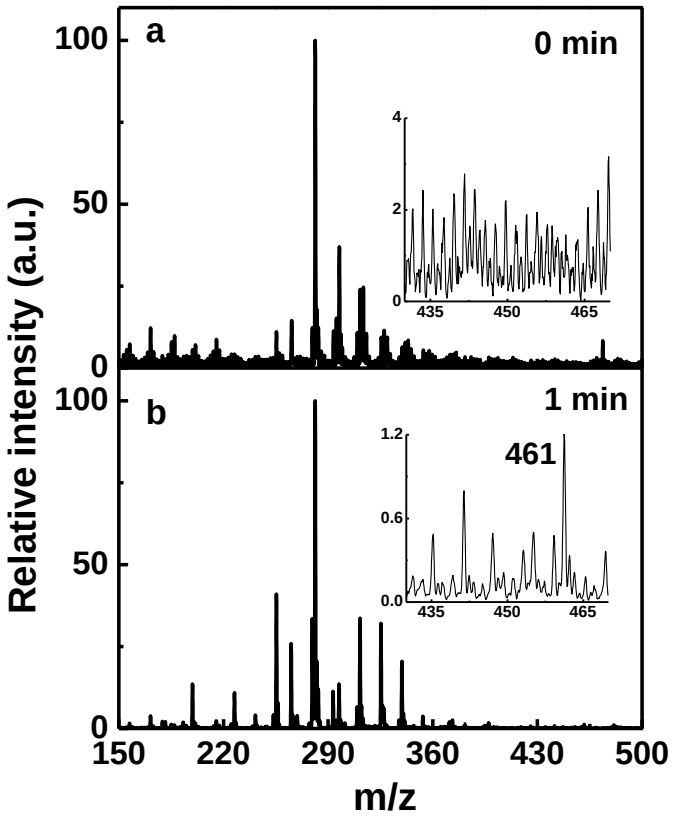

Figure S4. Mass spectra collected from the aqueous phase a) after bulk reaction and b) after 1 min of sonication. Insets of both Figures show the zoomed-in view of the selected mass range to display the peak intensity of m/z 461.

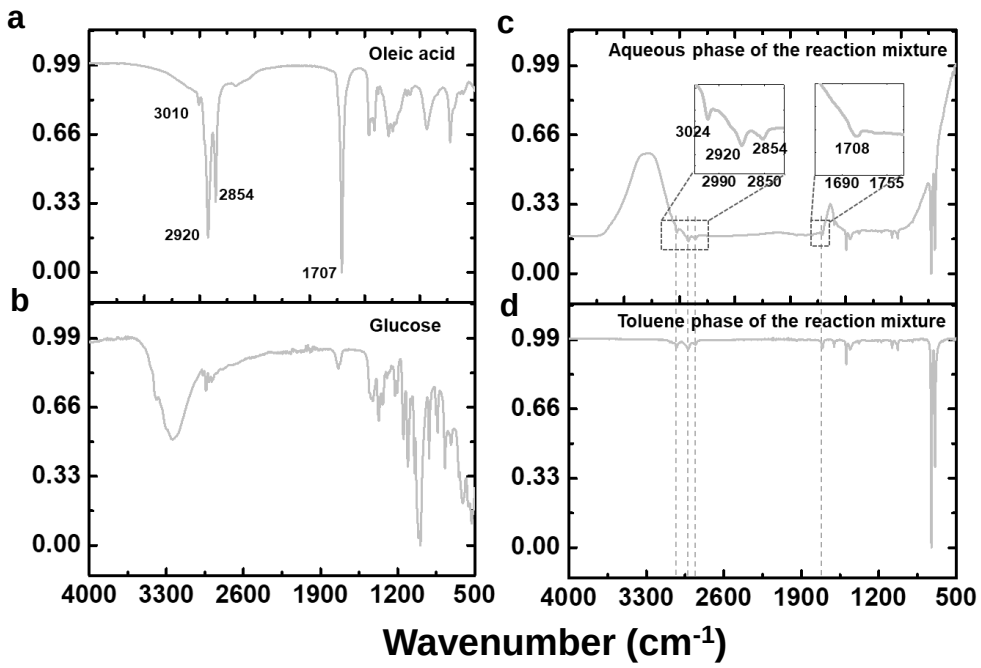

Figure S5. IR-spectra of a,b) standard oleic acid and glucose, and c,d) aqueous and toluene phase after extraction, showing the presence of oleic acid and toluene, respectively. Dotted lines in the aqueous and toluene phase indicate the characteristic peaks of oleic acid resulting from the CH stretch, asymmetric and symmetric stretches of CH_2, and C=O stretch at 3010, 2926, 2854, and 1707 cm^{-1}, respectively, suggesting the presence of oleic acid in aqueous solution.

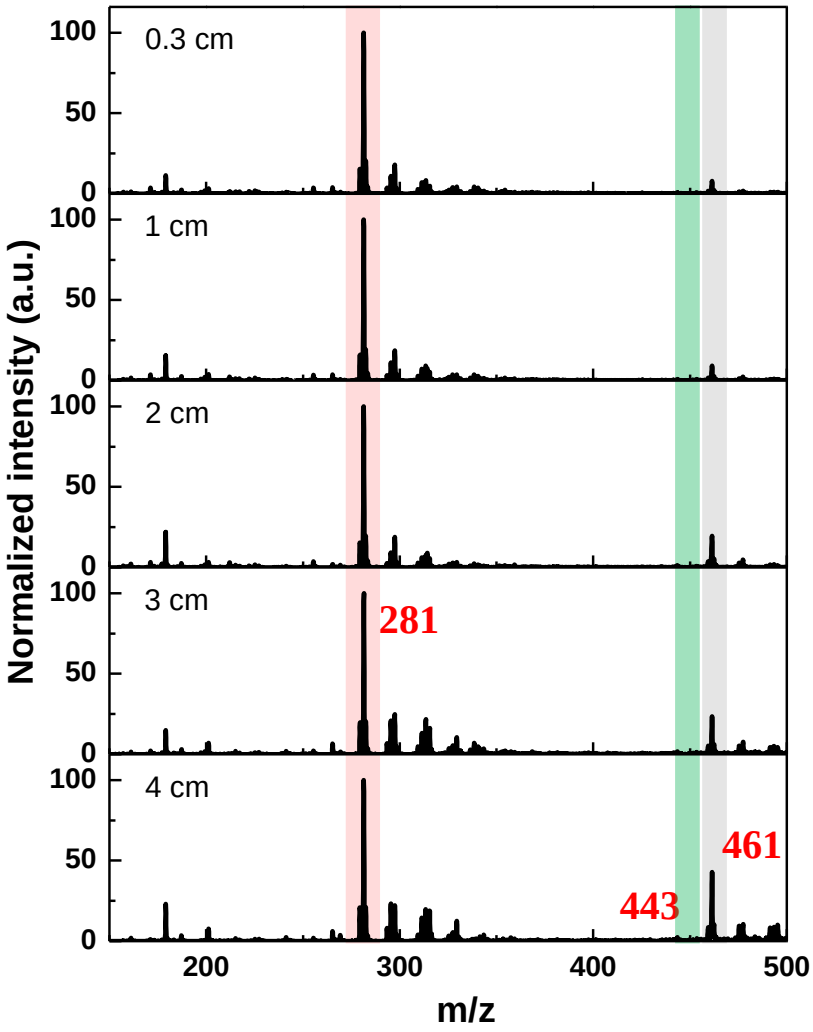

Figure S6. Distance dependence mass spectra of glucose/oleic acid reaction mixture. Red, green, and grey shades indicate the peak positions for deprotonated oleic acid, product, and intermediate, respectively.

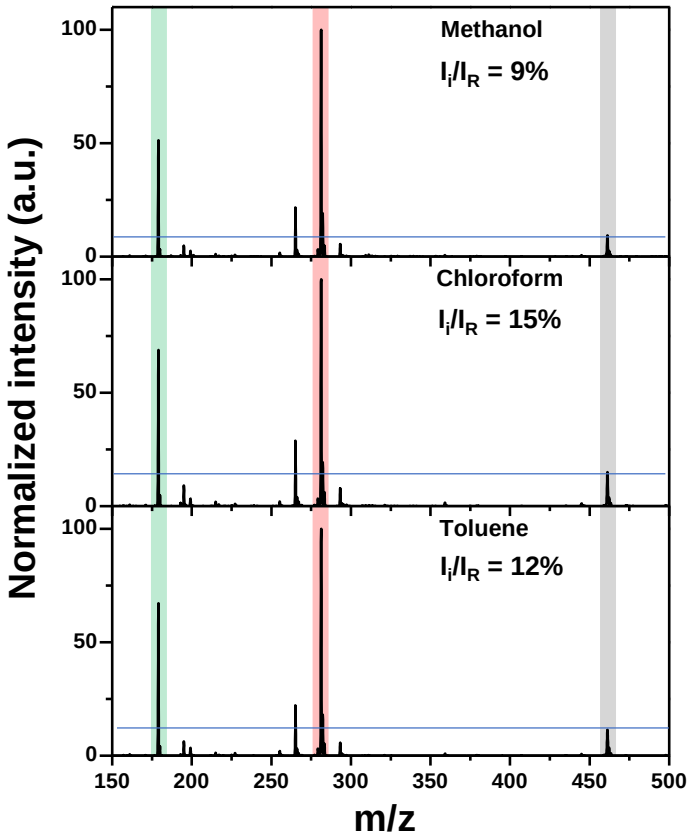

Figure S7. Mass spectra of reaction mixtures in methanol, chloroform, and toluene, showing better reaction yield in a nonpolar solvent system in comparison to a polar solvent. Red, green and grey shades indicate the peak positions for deprotonated oleic acid, glucose, and intermediate, respectively. Higher relative ratio of the peak intensity (indicated by blue horizontal lines) in chloroform and toluene than that of methanol shows better reaction in the nonpolar medium.

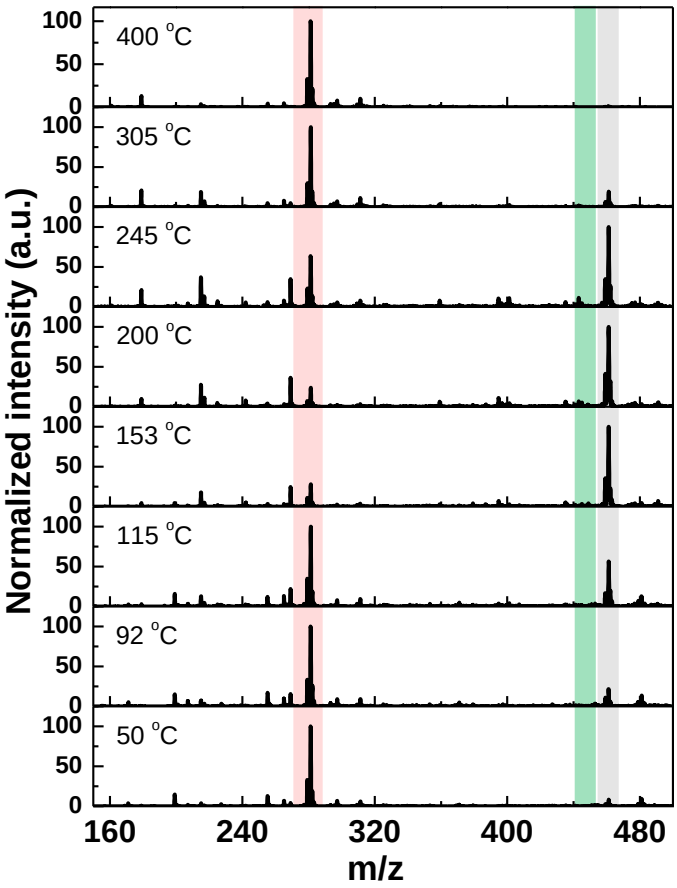

Figure S8. Temperature dependent mass spectra of glucose/oleic acid reactions. Red, green, and grey shades highlight the peak positions at m/z 281, 443, and 461, respectively.

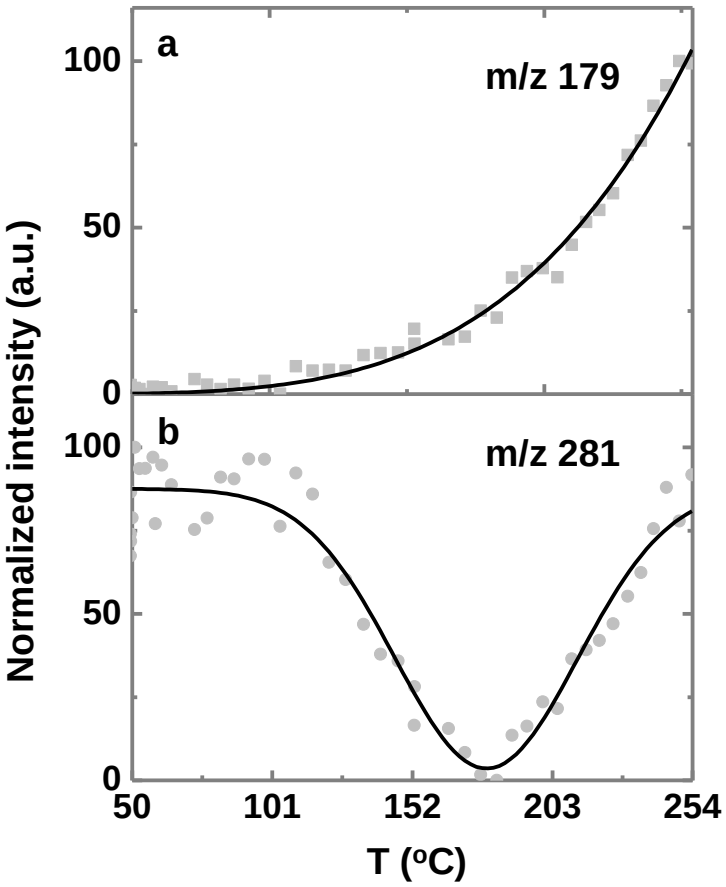

Figure S9. Ion intensity *Vs* temperature plot for a) glucose (m/z 179) and b) oleic acid (m/z 281).

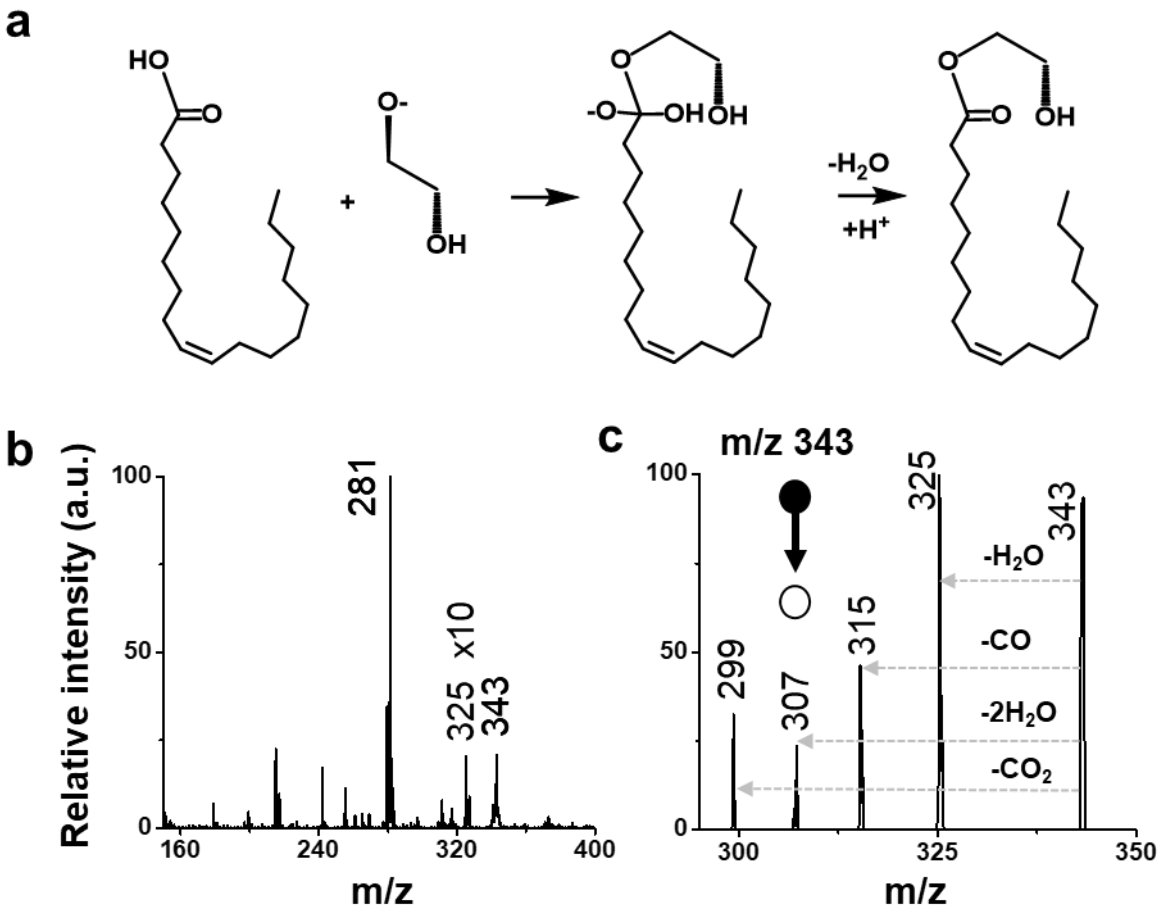

Figure S10. Microdroplet synthesis of ethylene glycol/oleic acid ester. A) Reaction scheme showing the formation of the tetrahedral intermediate and neutral product after a water loss. B) Full range mass spectrum of the microdroplet reaction showing peaks for reagent, product, and intermediate species at m/z 281, 325, and 343, respectively. Peak at m/z 325 is multiplied 10 times. Note that the additional peaks in the spectrum are due to chemical or electrical noise. C) MS/MS spectrum of the intermediate peak.

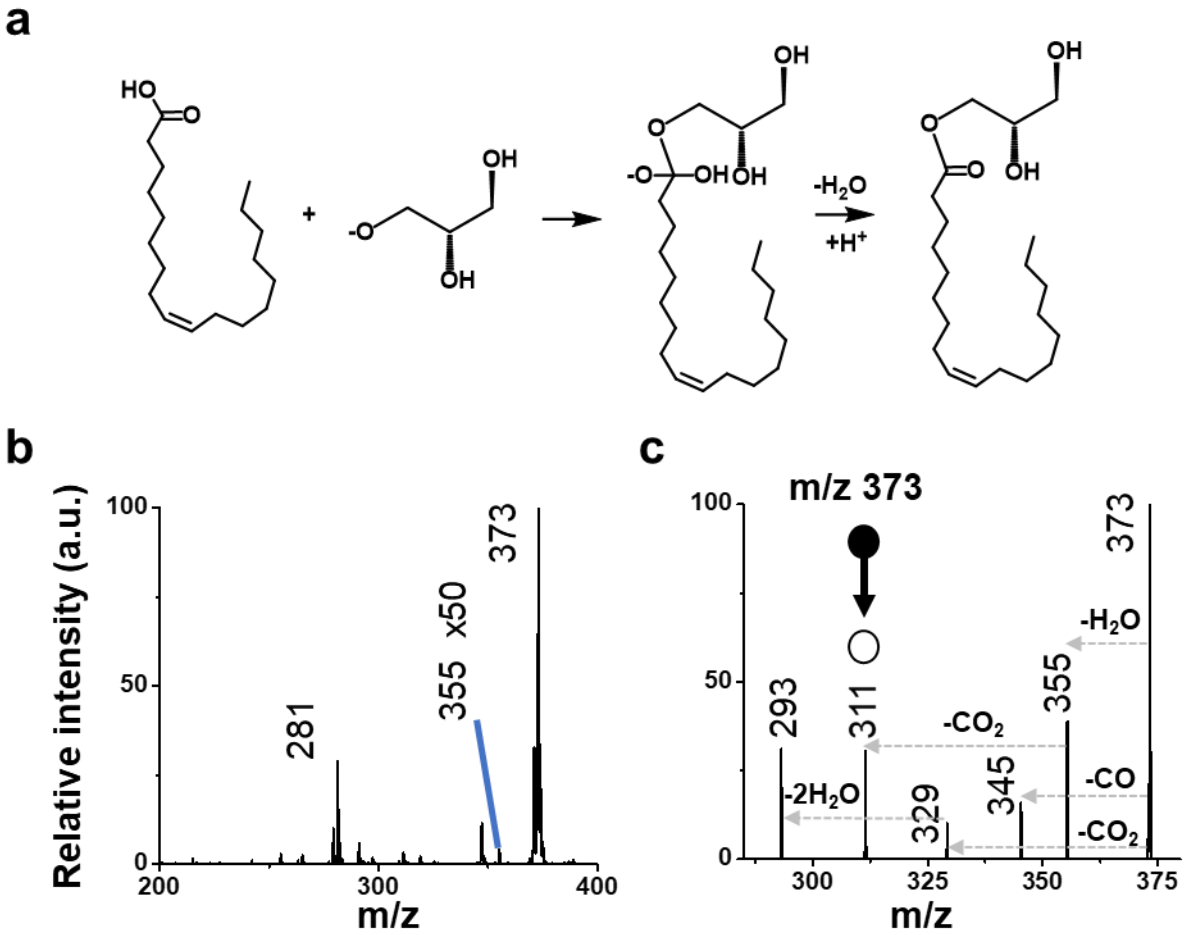

Figure S11. Microdroplet synthesis of glycerol/oleic acid ester. A) Reaction scheme showing the formation of the tetrahedral intermediate and neutral product after a water loss. B) Full range mass spectrum of the microdroplet reaction showing peaks for reagent, product and intermediate species at m/z 281, 355 and 373, respectively. Peak at m/z 335 is multiplied 50 times. Note that the additional peaks in the spectrum are due to chemical or electrical noise. C) MS/MS spectrum of the intermediate peak at m/z 373.

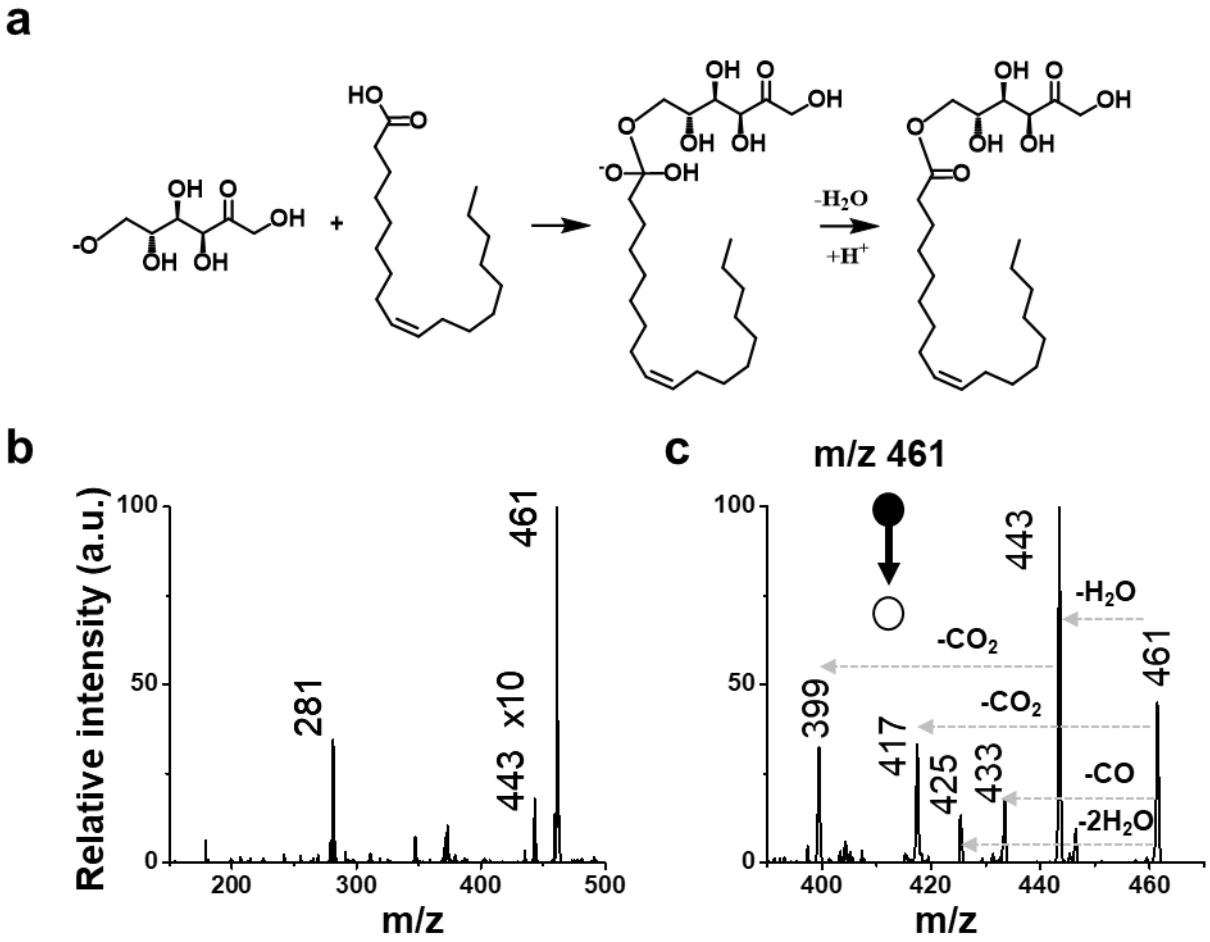

Figure S12. Microdroplet synthesis of fructose/oleic acid ester. A) Reaction scheme showing the formation of the tetrahedral intermediate and neutral product after a water loss. B) Full range mass spectrum of the microdroplet reaction showing deprotonated reagent, product, and intermediate peak at m/z 281, 443, and 461, respectively. Peak at m/z 443 is multiplied 10 times. Note that the other peaks in the spectrum are due to chemical or electrical noise. C) MS/MS spectrum of the intermediate peak at m/z 461.

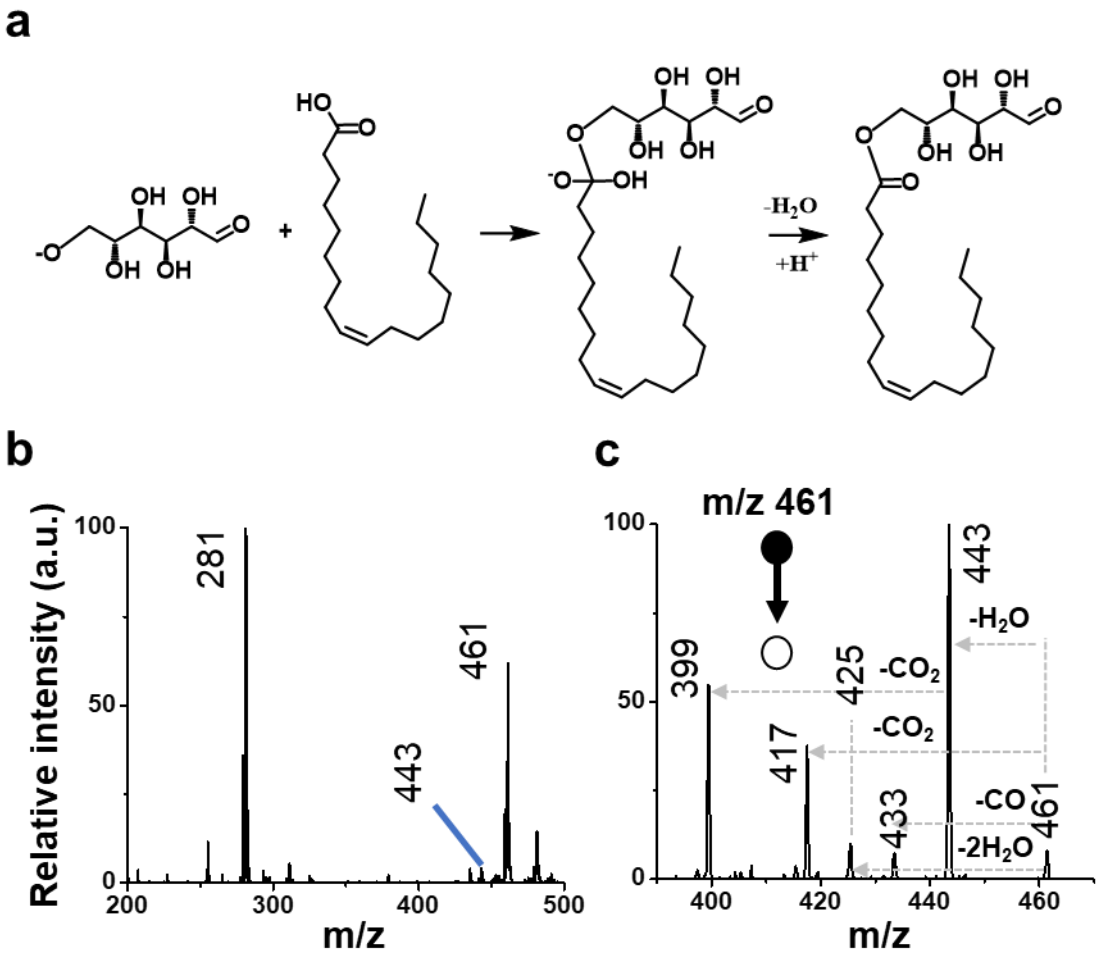

Figure S13. Microdroplet synthesis of mannose/oleic acid ester. A) Reaction scheme showing the formation of the tetrahedral intermediate and neutral product after a water loss. B) Full range mass spectrum of the microdroplet reaction showing deprotonated reagent, product, and intermediate peak at m/z 281, 443, and 461, respectively. Note that the other peaks in the spectrum are due to chemical or electrical noise. C) MS/MS spectrum of the intermediate peak at m/z 461.

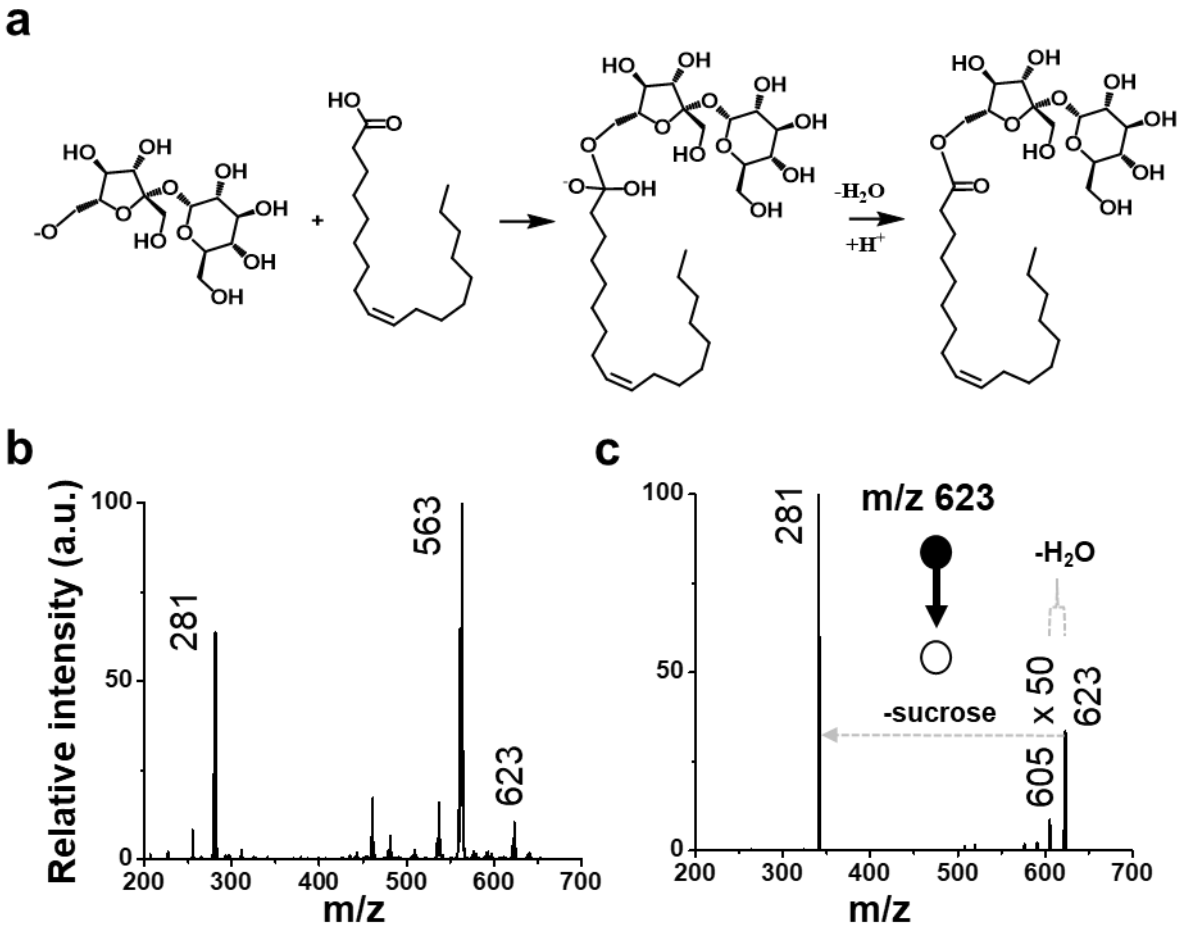

Figure S14. Microdroplet synthesis of glycerol/oleic acid ester. A) Reaction scheme showing the formation of the tetrahedral intermediate and neutral product after a water loss. B) Full range mass spectrum of the microdroplet reaction showing deprotonated reagent and intermediate peak at m/z 281 and 623, respectively. The base peak at m/z 563 corresponds to a dimer of oleic acid. Note that the other peaks in the spectrum are due to chemical or electrical noise. C) MS/MS spectrum of the intermediate peak at m/z 623. Peak at m/z 605 is multiplied 50 times.

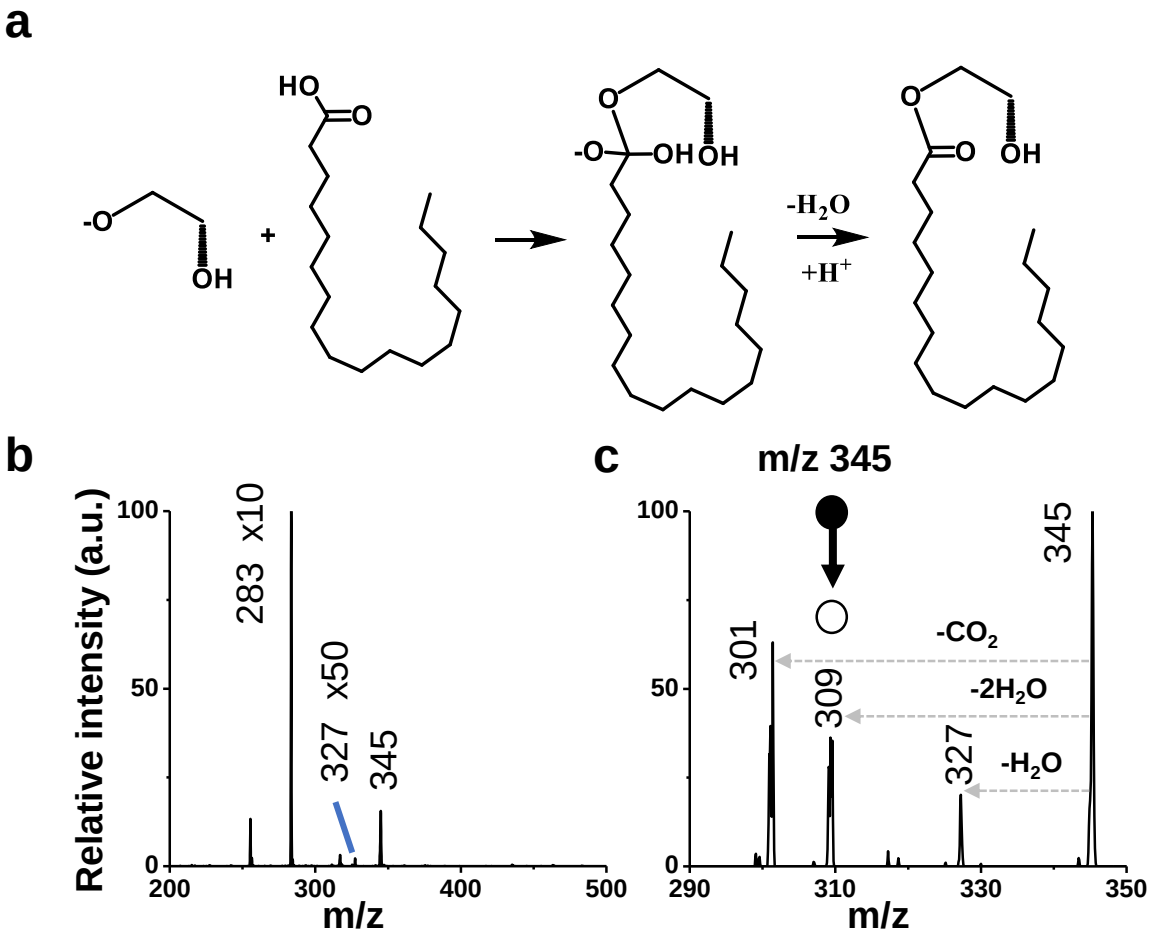

Figure S15. Microdroplet synthesis of ethylene glycol/stearic acid ester. A) Reaction scheme showing the formation of the tetrahedral intermediate and neutral product after a water loss. B) Full range mass spectrum of the microdroplet reaction showing deprotonated reagent, product, and intermediate peak at m/z 281, 327, and 345, respectively. Peaks at m/z 283 and 327 are multiplied 10 and 50 times. Note that the other peaks in the spectrum are due to chemical or electrical noise. C) MS/MS spectrum of the intermediate at m/z 345.

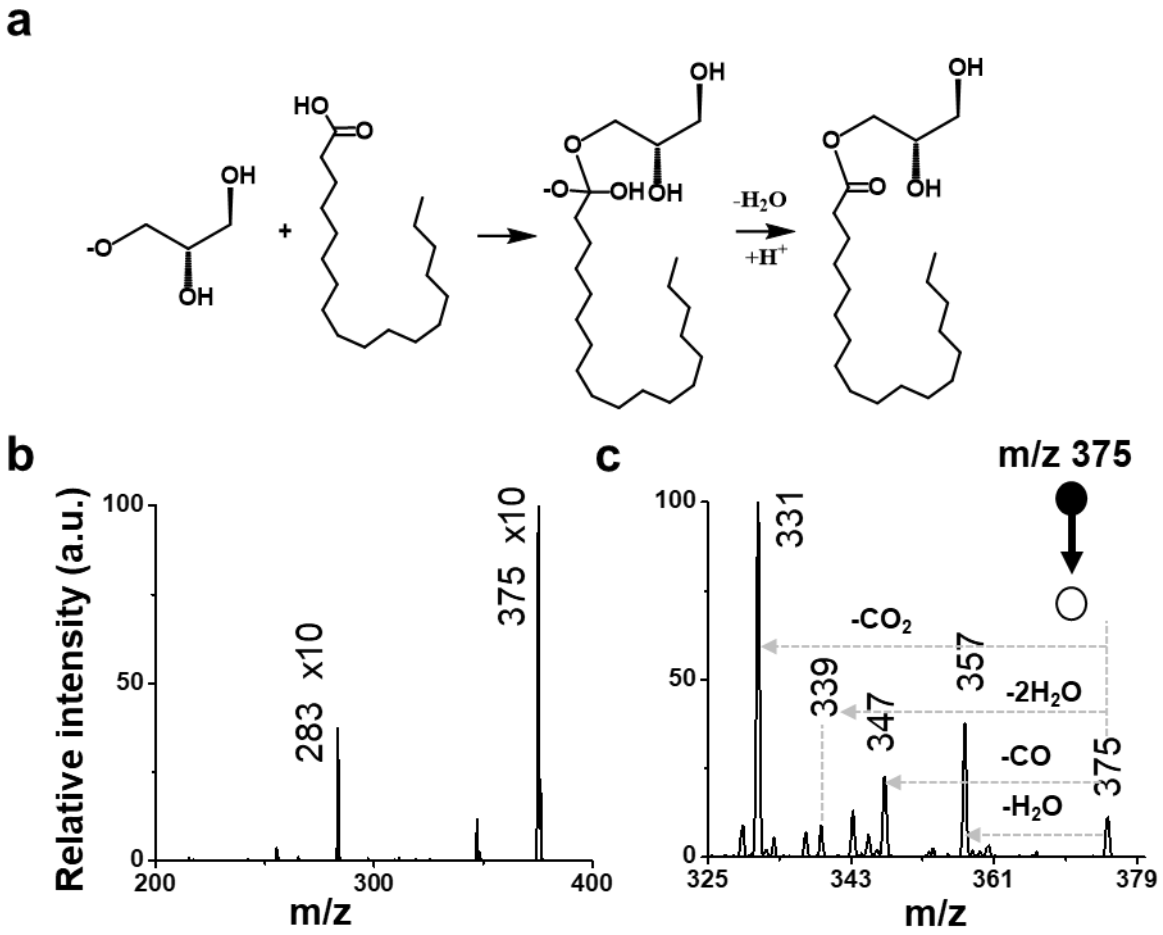

Figure S16. Microdroplet synthesis of glycerol/stearic acid ester. A) Reaction scheme showing the formation of the tetrahedral intermediate and neutral product after a water loss. B) Full range mass spectrum of the microdroplet reaction showing deprotonated reagent and intermediate peak at m/z 281 and 375, respectively. Peaks are multiplied 10 times. Note that the other peaks in the spectrum are due to chemical or electrical noise. C) MS/MS spectrum of the intermediate at m/z 375.

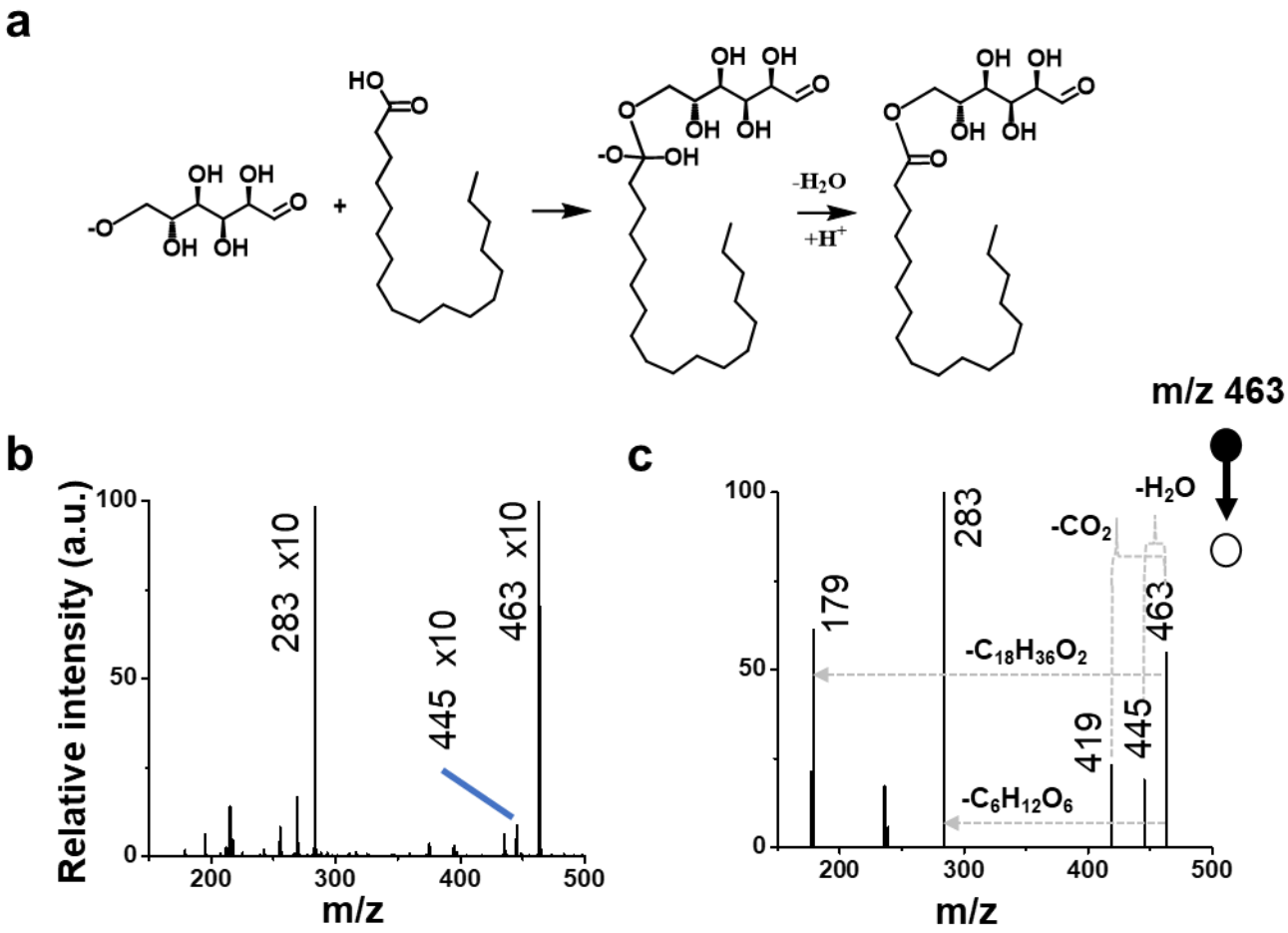

Figure S17. Microdroplet synthesis of glucose/stearic acid ester. A) Reaction scheme showing the formation of the tetrahedral intermediate and neutral product after a water loss. B) Full range mass spectrum of the microdroplet reaction showing deprotonated reagent, product, and intermediate peak at m/z 281, 445, and 463, respectively. Peaks are multiplied 10 times. Note that the other peaks in the spectrum are due to chemical or electrical noise. C) MS/MS spectrum of the intermediate at m/z 463.

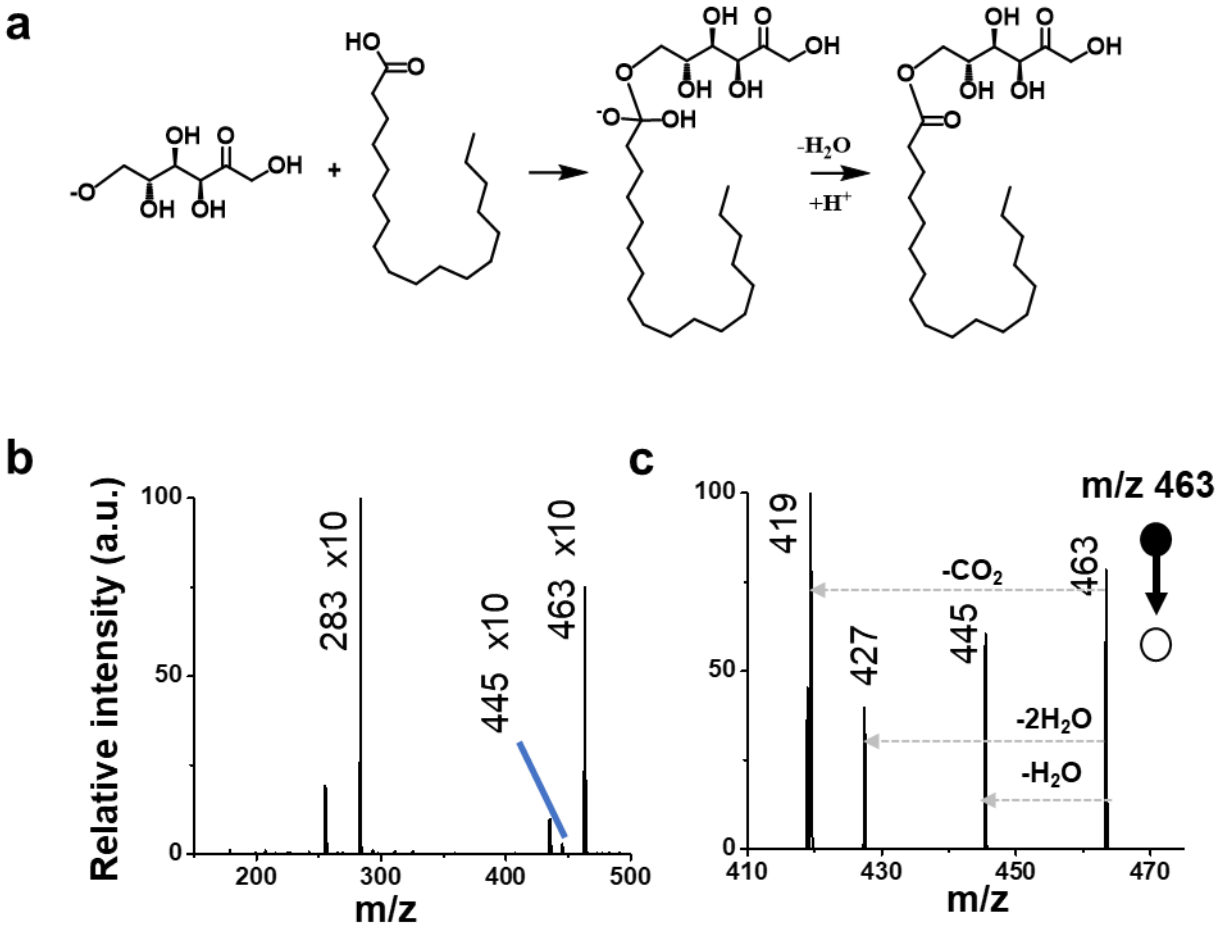

Figure S18. Microdroplet synthesis of fructose/stearic acid ester. A) Reaction scheme showing the formation of the tetrahedral intermediate and neutral product after a water loss. B) Full range mass spectrum of the microdroplet reaction showing deprotonated reagent, product, and intermediate peak at m/z 281, 445, and 463, respectively. Peaks are multiplied 10 times. Note that the other peaks in the spectrum are due to chemical or electrical noise. C) MS/MS spectrum of the intermediate at m/z 463.

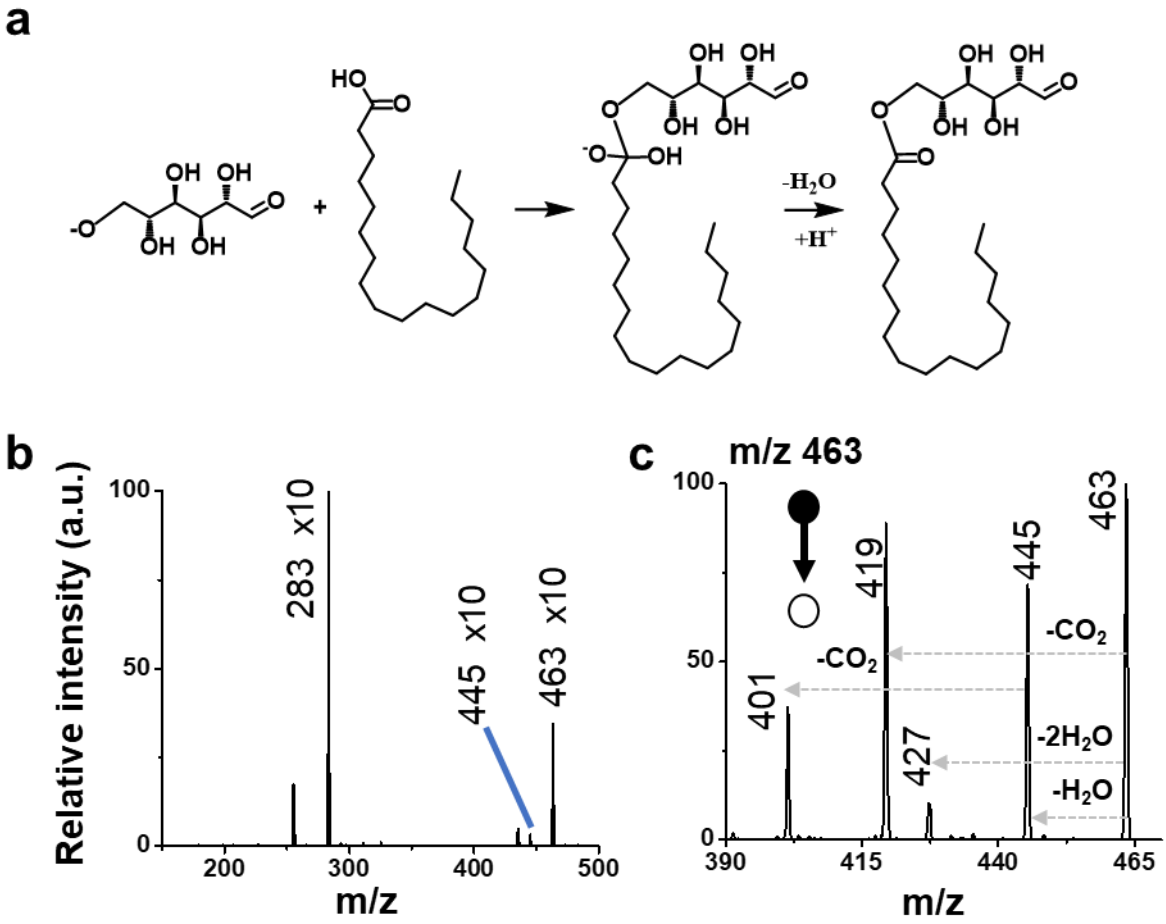

Figure S19. Microdroplet synthesis of mannose/stearic acid ester. A) Reaction scheme showing the formation of the tetrahedral intermediate and neutral product after a water loss. B) Full range mass spectrum of the microdroplet reaction showing deprotonated reagent, product, and intermediate peak at m/z 281, 445, and 463, respectively. Peaks are multiplied 10 times. Note that the other peaks in the spectrum are due to chemical or electrical noise. C) MS/MS spectrum of the intermediate at m/z 463.

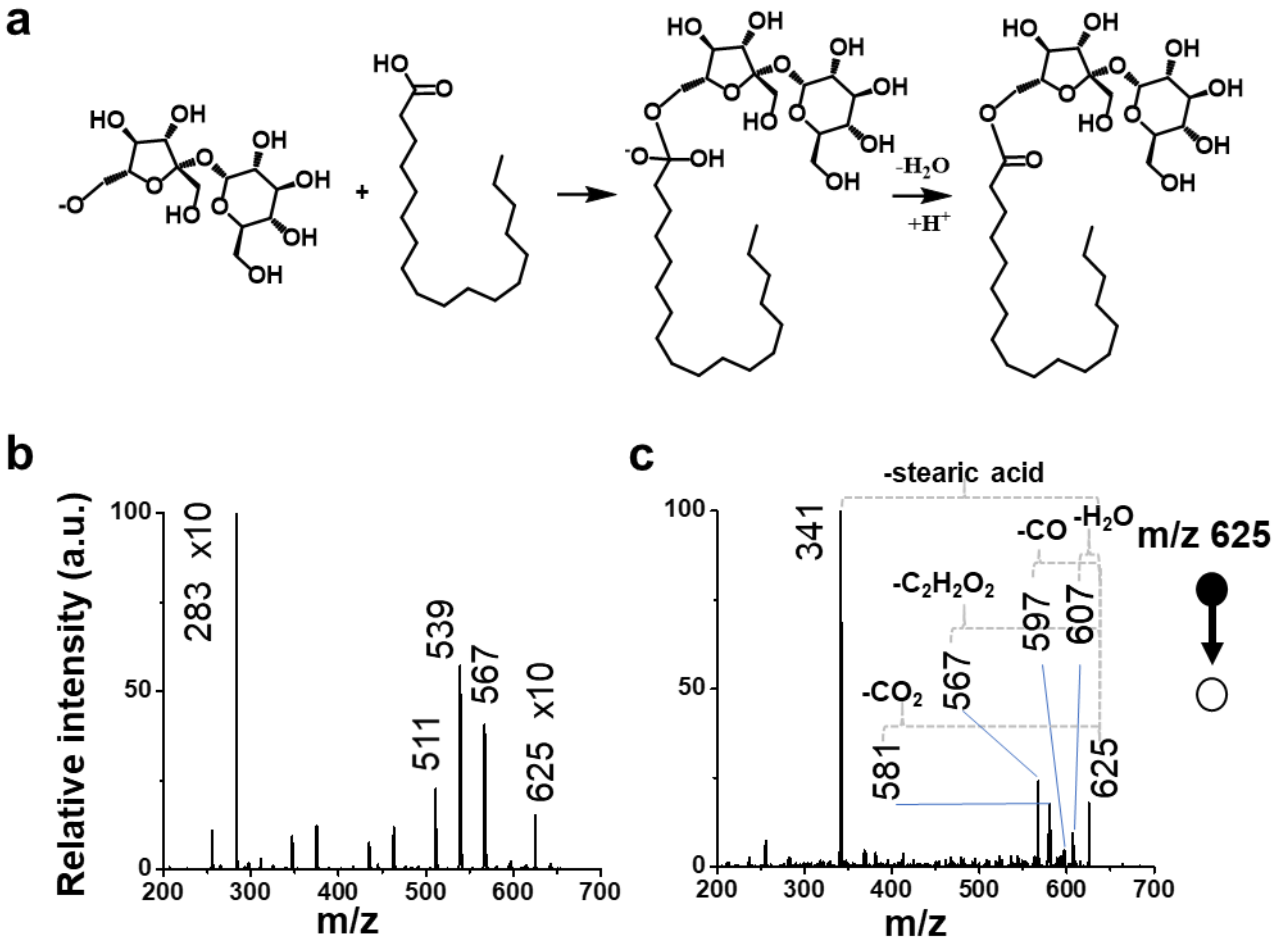

Figure S20. Microdroplet synthesis of sucrose/stearic acid ester. A) Reaction scheme showing the formation of the tetrahedral intermediate and neutral product after a water loss. B) Full range mass spectrum of the microdroplet reaction showing deprotonated reagent, product, and intermediate peak at m/z 281, 325, and 343, respectively. Peaks at m/z 283 and 625 are multiplied 10 times. Note that the peak at m/z 567 corresponds to the dimer of stearic acid. The other two peaks at m/z 511 and 539 were either fragmented species or chemical contamination. Peaks with lower intensity in the spectrum are due to chemical or electrical noise. C) MS/MS spectrum of the intermediate at m/z 625.

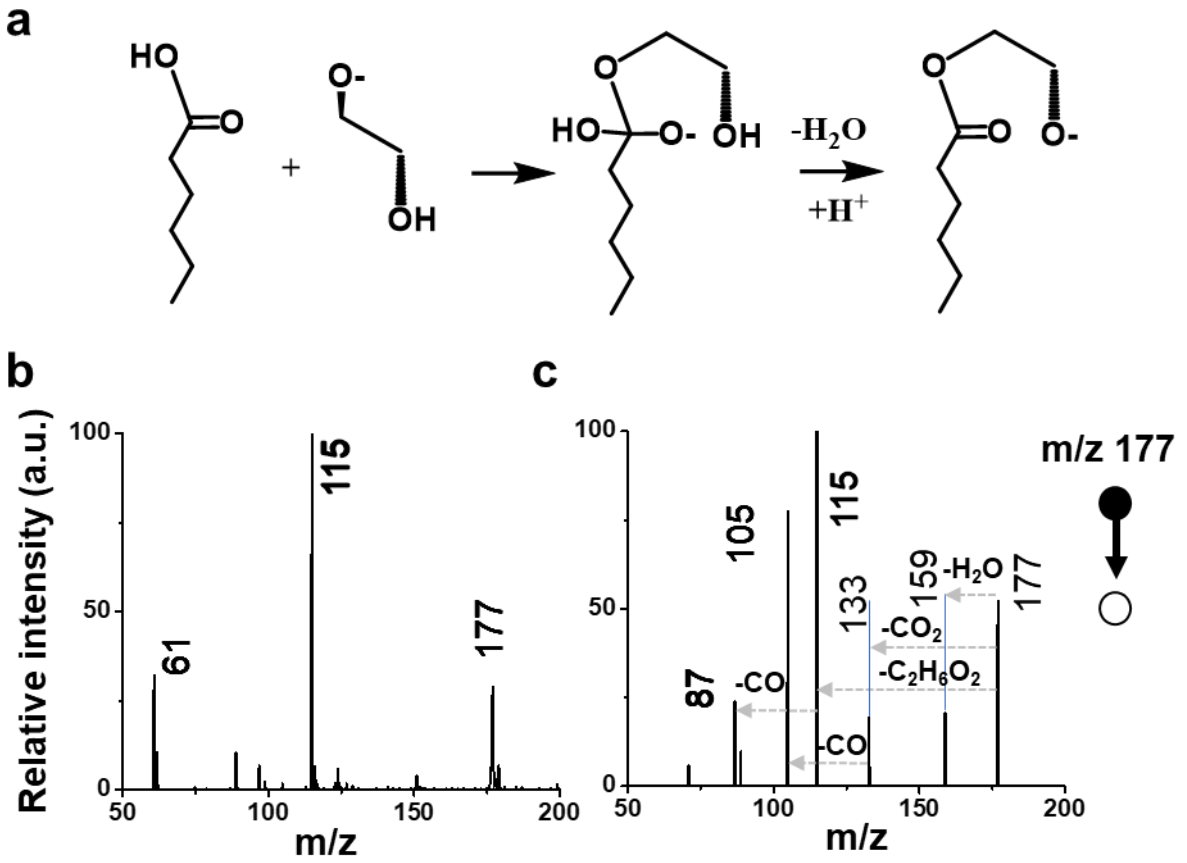

Figure S21. Microdroplet synthesis of ethylene glycol/caproic acid ester. A) Reaction scheme showing the formation of the tetrahedral intermediate and neutral product after a water loss. B) Full range mass spectrum of the microdroplet reaction showing deprotonated reagents and intermediate peak at m/z 61, 115, and 117, respectively. Note that the other peaks in the spectrum are due to chemical or electrical noise. C) MS/MS spectrum of the intermediate at m/z 117.

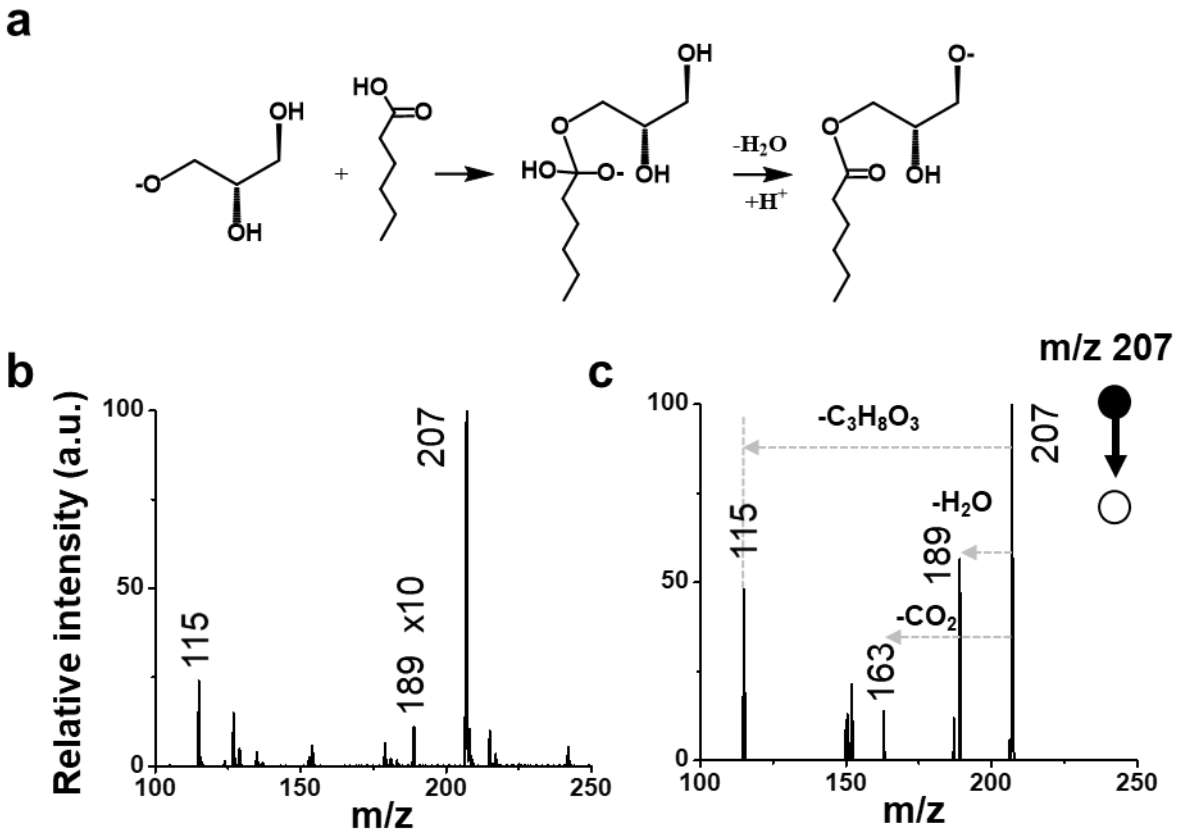

Figure S22. Microdroplet synthesis of gycerol/caproic acid ester. A) Reaction scheme showing the formation of tetrahedral intermediate and neutral product after water loss. B) Full range mass spectrum of the microdroplet reaction showing deprotonated reagent, product, and intermediate peak at m/z 115, 189, and 207, respectively. Peak at m/z 189 is multiplied 10 times. Note that the other peaks in the spectrum are due to chemical or electrical noise. C) MS/MS spectrum of the intermediate at m/z 207.

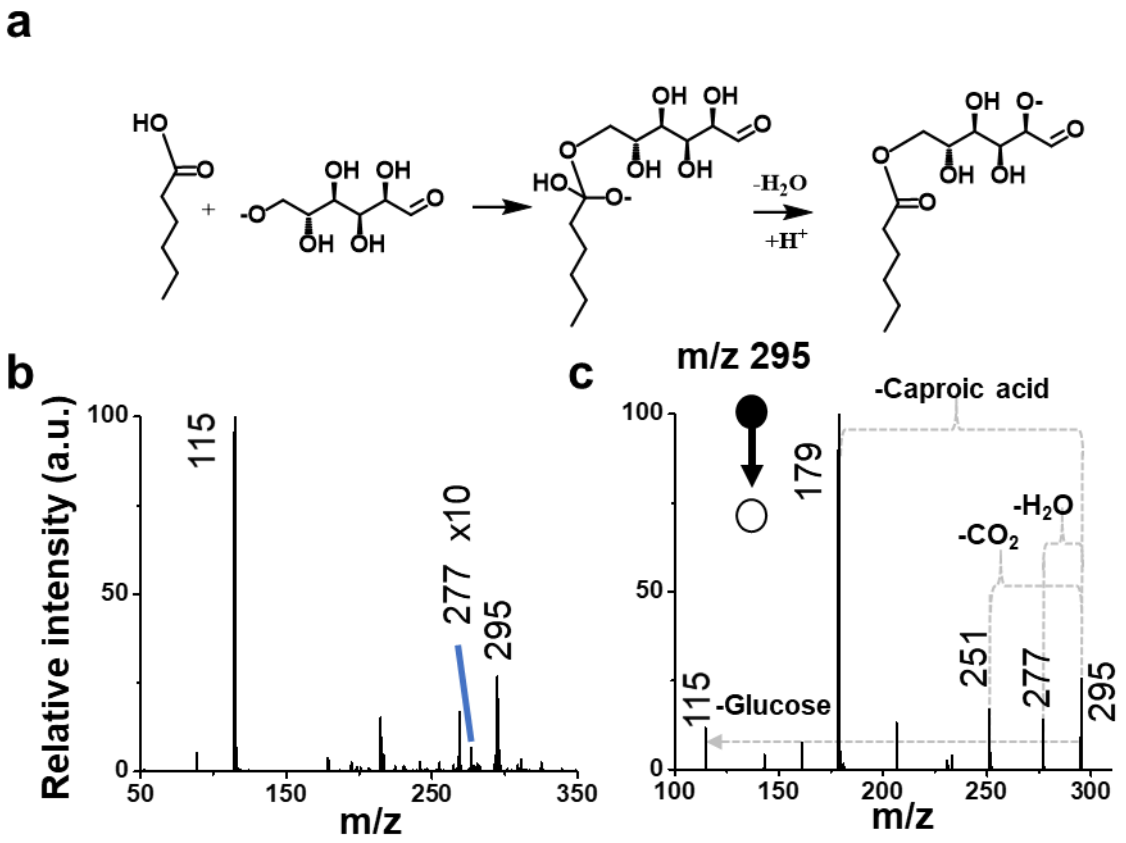

Figure S23. Microdroplet synthesis of glucose/caproic acid ester. A) Reaction scheme showing the formation of the tetrahedral intermediate and neutral product after a water loss. B) Full range mass spectrum of the microdroplet reaction showing deprotonated reagent, product, and intermediate peak at m/z 115, 277, and 295, respectively. Peak at m/z 227 is multiplied 10 times. Note that the other peaks in the spectrum are due to chemical or electrical noise. C) MS/MS spectrum of the intermediate at m/z 295.

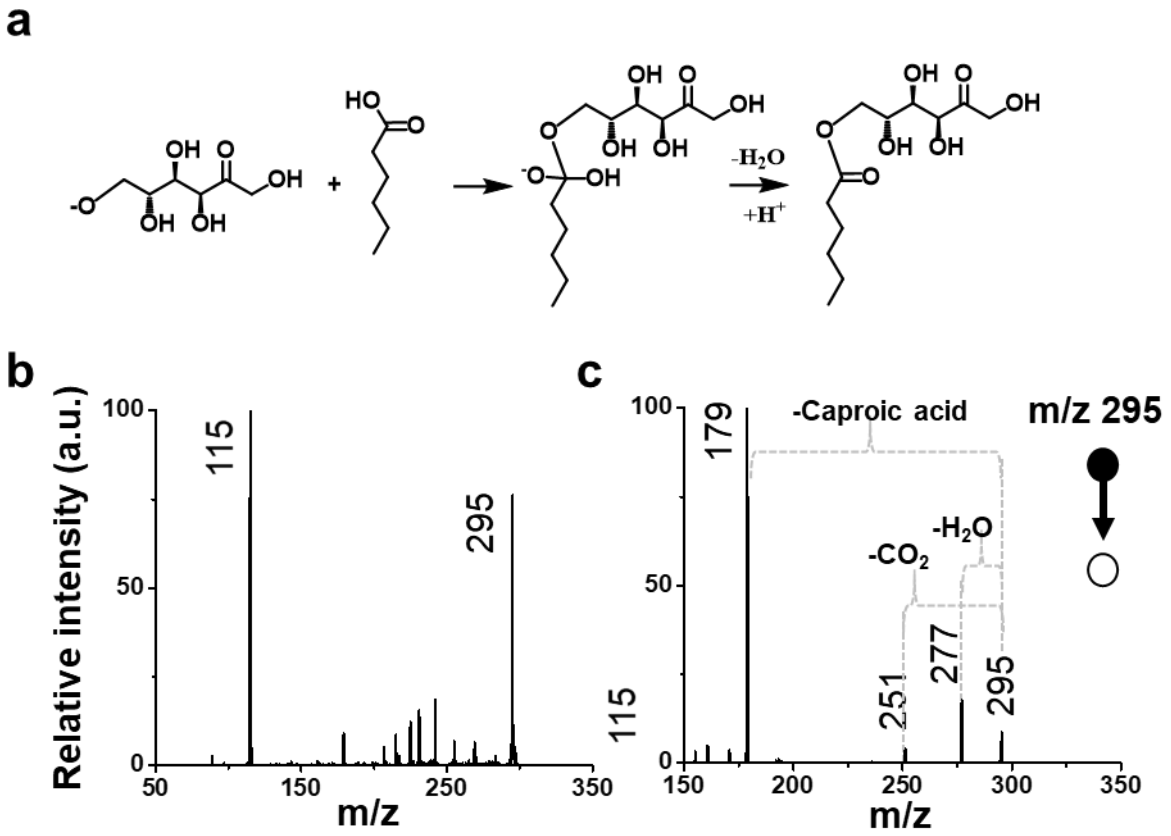

Figure S24. Microdroplet synthesis of fructose/caproic acid ester. A) Reaction scheme showing the formation of the tetrahedral intermediate and neutral product after a water loss. B) Full range mass spectrum of the microdroplet reaction showing deprotonated reagent and intermediate peak at m/z 115 and 295, respectively. Note that the other peaks in the spectrum are due to chemical or electrical noise. C) MS/MS spectrum of the intermediate at m/z 295.

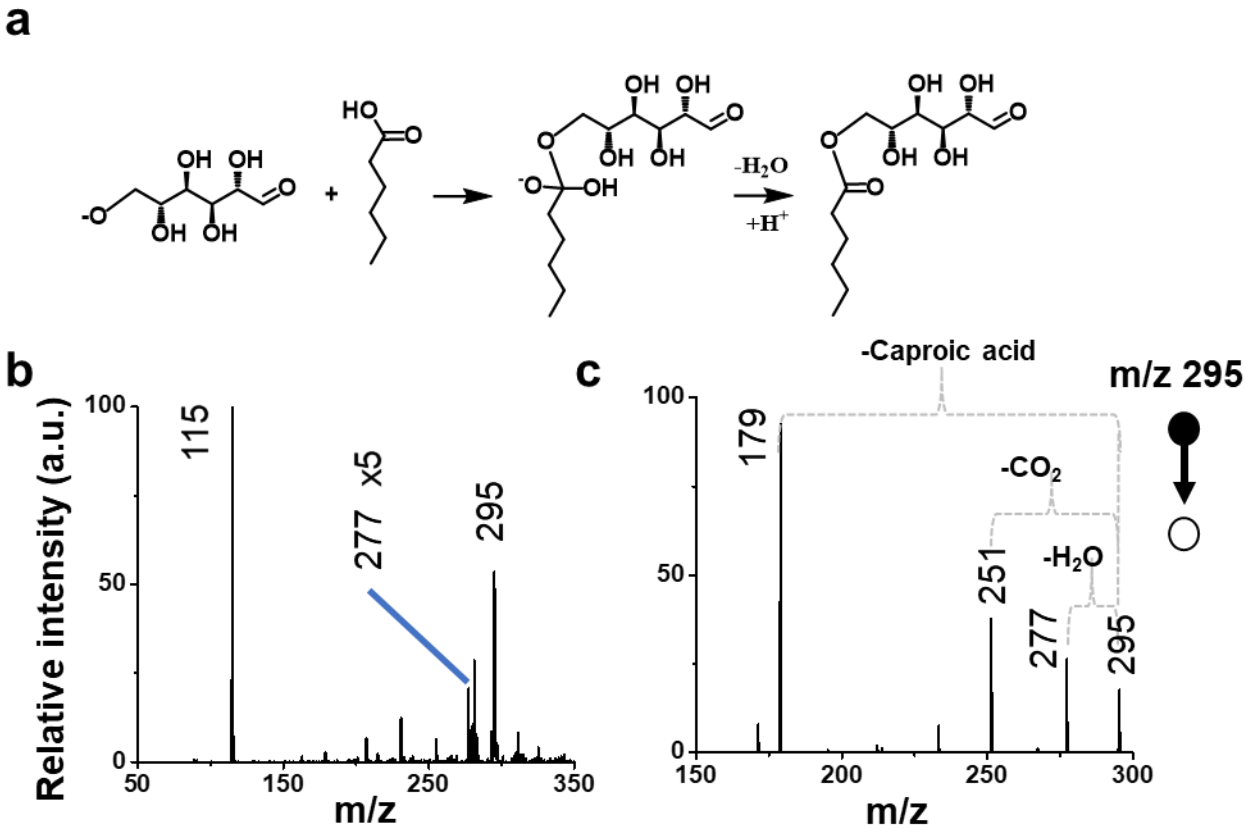

Figure S25. Microdroplet synthesis of mannose/caproic acid ester. A) Reaction scheme showing the formation of the tetrahedral intermediate and neutral product after a water loss. B) Full range mass spectrum of the microdroplet reaction showing deprotonated reagent, product, and intermediate peak at m/z 115, 277, and 295, respectively. Peak at m/z 227 is multiplied 5 times. Note that the other peaks in the spectrum are due to chemical or electrical noise. C) MS/MS spectrum of the intermediate at m/z 295.

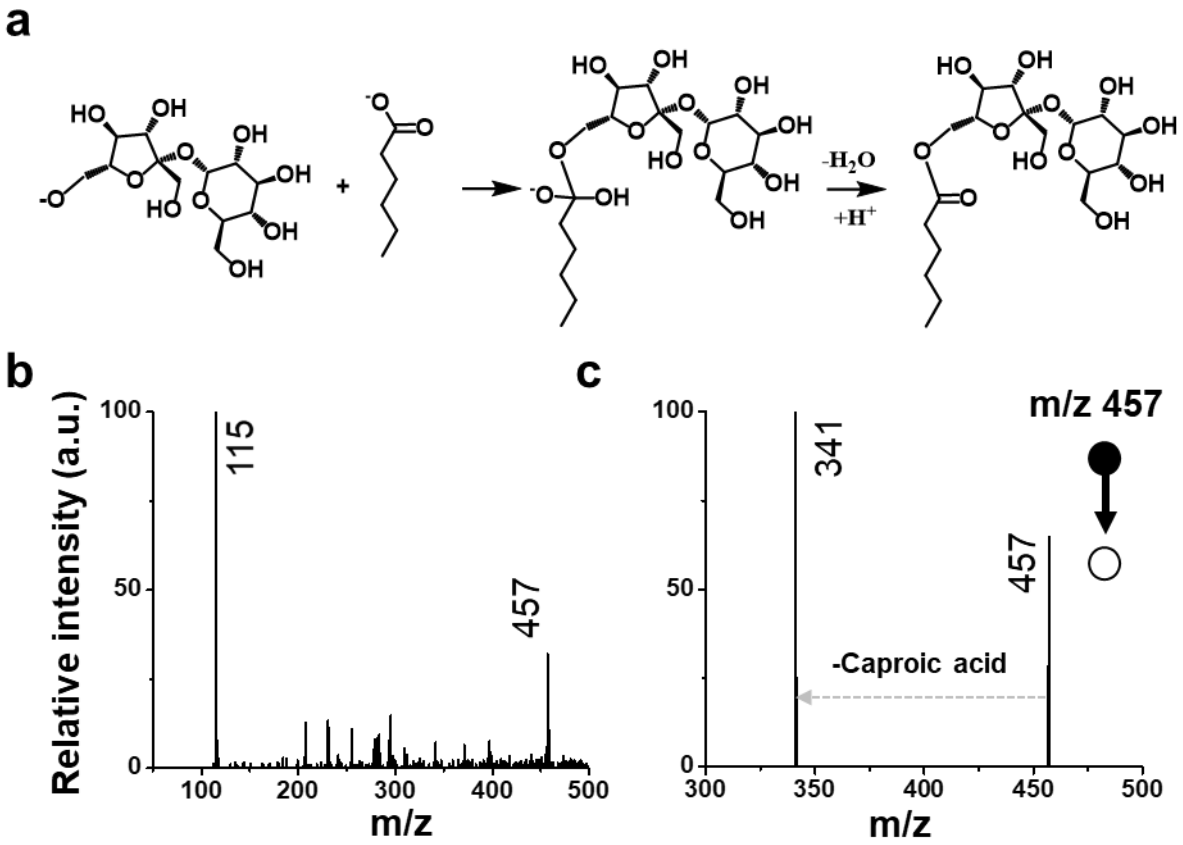

Figure S26. Microdroplet synthesis of sucrose/caproic acid ester. A) Reaction scheme showing the formation of the tetrahedral intermediate and neutral product after a water loss. B) Full range mass spectrum of the microdroplet reaction showing deprotonated reagent and intermediate peak at m/z 115 and 457, respectively. Note that the other peaks in the spectrum are due to chemical or electrical noise. C) MS/MS spectrum of the intermediate at m/z 457.